

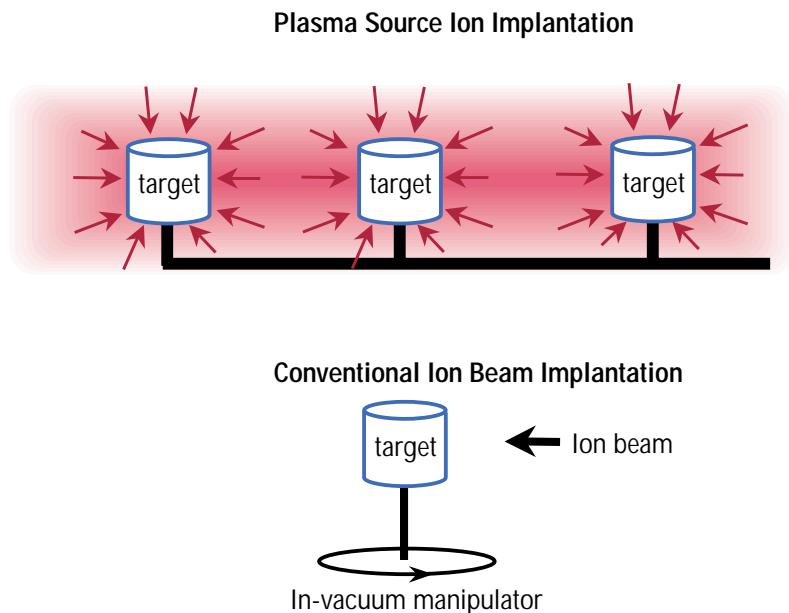
## Plasma Source Ion Implantation Research, Development, and Applications

*C. P. Munson, B. Cluggish (currently at Archimedes, San Diego), and B. Wood (P-24); and Kevin Walter (MST-8)*

### Introduction

Plasma Source Ion Implantation (PSII) is a room temperature, plasma-based, surface enhancement technology that uses an ionized gas surrounding a target and high-negative-voltage, high-current pulses to accelerate ions into a target surface from all directions. Ion implantation can modify the target surface in beneficial ways, making it harder, reducing the coefficient of friction, and enhancing its resistance to corrosion.<sup>1,2,3,4,5,6,7,8,9,10</sup> These benefits are similar to those obtained through conventional ion beam implantation<sup>11,12</sup>, but PSII differs from conventional techniques in several important aspects (see Fig. 1). First, ions are accelerated into the target through a plasma sheath<sup>13</sup> that surrounds the target, so the process is not “line-of-sight”—there is no requirement of an unobstructed path from a single ion source to the surface being treated. This allows PSII to treat multiple target surfaces and even multiple targets simultaneously without the need for in-vacuum manipulation of the target assembly. In addition, the average ion current to the target surface can be more than an order of magnitude larger than using conventional techniques<sup>14,15,16</sup>, significantly reducing the required treatment time for large, complex target assemblies. This increase in average ion current is possible because nearly the entire target surface (potentially many square meters in area) can be treated simultaneously with a high pulsed-current source. Spreading the total applied current over a large surface area also tends to minimize local surface heating effects.

*Fig. 1 Schematic comparison of PSII and conventional ion beam implantation. PSII uses the plasma sheath to accelerate ions into the target (or multiple targets) from all directions. Conventional, accelerator-based ion implantation is a line-of-sight process, which requires in-vacuum manipulation of a target to implant complex surfaces.*



PSII was originally patented by John Conrad of the University of Wisconsin, Madison, and has been further developed and demonstrated at industrially relevant scales by researchers at Los Alamos in collaboration with the University of Wisconsin and General Motors Research. This technique is currently being commercialized through the efforts of General Motors, Asea Brown Boveri, Litton Electron Devices, Nano Instruments, Diversified



*Fig. 2 The Los Alamos team participating in development and commercialization of PSII included (from left to right) Carter Munson, Michael Nastasi, Donald Rej, Jay Scheuer, Blake Wood, Kevin Walter, Ricky Faehl, and Ivars Henins. Team members not pictured include William Reass, Darrell Roybal, and Jose Garcia.*

Technologies, Ionex, PVI, Empire Hard Chrome, A. O. Smith, Harley-Davidson, Kwikset, Boeing, and DuPont, as well as Los Alamos National Laboratory and the University of Wisconsin at Madison in a National Institute of Standards and Technology Advanced Technology Program project managed by the Environmental Institute of Michigan, Ann Arbor. The success of this research and development (R&D) effort earned an R&D 100 award from *R&D Magazine* in 1996 (Fig. 2).

There are several key factors that must be considered to successfully design and operate a commercial PSII system. These include the surface material science, overall vacuum system design, plasma source requirements, plasma-target interaction considerations, pulsed high-voltage subsystem (modulator) requirements, and target requirements and limitations. Critical system components are outlined in Fig. 3. This research highlight will focus on several important plasma physics effects related to the plasma-target interaction, particularly in the case of large, complex, multiple-component, target assemblies.

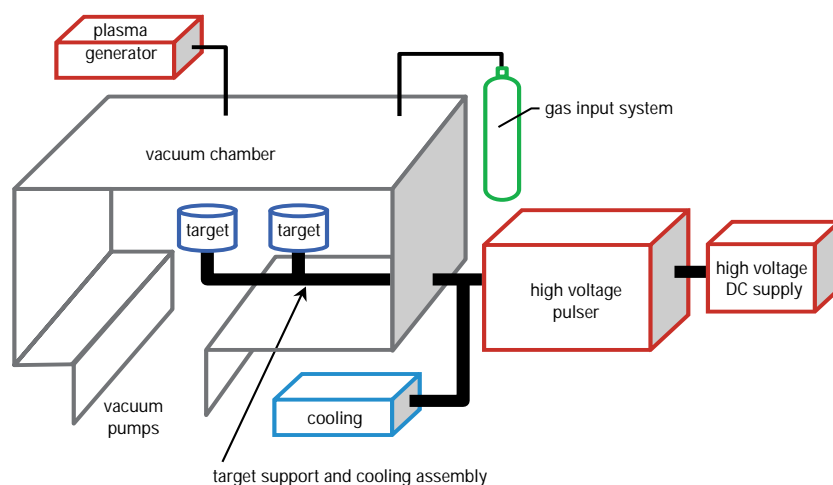


*Fig. 3 Block diagram of a typical PSII system. Major system components include the vacuum chamber, pumping system, high voltage DC power supply, high voltage pulser or modulator, cooling system, target support assembly, plasma generation system, and working gas input system.*

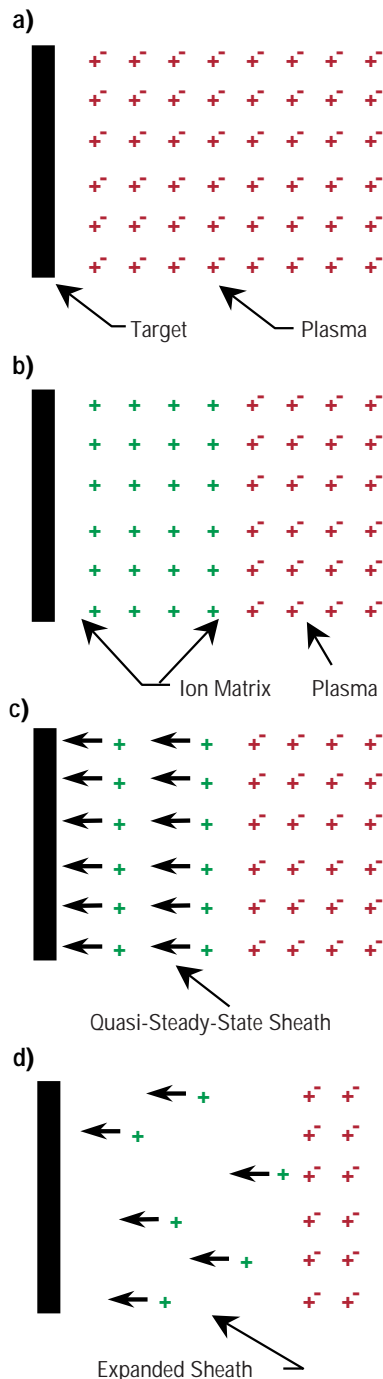


*Fig. 4 Plasma sheath temporal behavior for a planar target. Shown are the initial configuration with nearly uniform plasma surrounding the target (a), the formation of the ion matrix after electrons have been excluded from the region close to the target (b), ions accelerating through the sheath region into the target surface (c), and the expanded sheath late in the voltage pulse (d).*

### Basic Plasma Sheath Physics

During the PSII process, a negative high voltage pulse is applied to create a transient plasma sheath<sup>17,18,19</sup> around the target and accelerate ions into the target surface. The characteristics of the plasma sheath play a major role in the PSII process. The fundamental evolution of the plasma sheath is illustrated in Fig. 4. In simple configurations (uniform plasma density and geometrically simple targets) the dimensions of the sheath are determined primarily by the initial plasma density, the voltage applied to the target, and the duration of the voltage pulse. In the basic initial configuration (Fig. 4a) a nearly uniform plasma surrounds the target. The great difference in mass between the electrons and ions in the plasma causes the electrons to move rapidly away from the target during the early portion of the voltage pulse, exposing plasma ions (Fig. 4b). The electric field established in the sheath region accelerates ions into the target (Fig. 4c). As ions are implanted into the target and lost from the sheath, the sheath edge recedes from the target (Fig. 4d). The sheath thickness increases during this time. Eventually, the sheath edge will extend to the vacuum chamber wall, or arcing will occur, limiting the useful pulse duration for implantation. Typical pulse widths, therefore, range from several microseconds to almost 100  $\mu$ s.

From the fundamental equations describing the sheath evolution, it is clear that higher initial plasma densities result in smaller sheaths. Sheath dimensions that are small compared to the scale size of important target features result in more uniform implantation of the critical target surfaces, but require larger currents from the modulator.

### Plasma Sheath and Target Interactions

A serious factor affecting PSII's commercial success is the production of secondary electrons.<sup>8</sup> Secondary electrons are produced when plasma ions impact the target surface, with each high-energy (many keV) ion potentially displacing a large number of electrons upon impact. For an aluminum target biased to 40 kV, as many as 19 secondary electrons are produced by each ion.<sup>20</sup> This would indicate an ion implantation efficiency of only 5% for the PSII process, since the total current that must be supplied by the modulator is composed of both the ion and secondary electron currents.

Under certain circumstances, the secondary electrons, rather than being a nuisance, may actually enhance the plasma discharge. The secondary electrons are repelled by the strong negative potential of the target and are accelerated to high energy in their outward passage through the sheath surrounding the target. When multiple, large, complex target assemblies are being treated with PSII, secondary electrons emitted by one portion of the target may be reflected from the sheath edge associated with other portions of the target surface, resulting in an increase in the residence time of the secondaries in the plasma. A larger portion of the energy of the



*Fig. 5 Image of the target assembly consisting of ~1,000 piston surrogates in a background argon plasma.*

secondary electrons is then deposited into the plasma, producing increased ionization and higher plasma densities than could be achieved without the secondaries.

Figure 5 shows the target assembly used in our experiments immersed in a background plasma. The assembly consists of four vertical racks consisting of 504 cylindrical targets (surrogates for aluminum automotive pistons). Each surrogate piston is a 5.08-cm-long section of 8.25-cm-diameter aluminum alloy tubing. The surrogate pistons are mounted lengthwise in pairs with a thin aluminum cap on each end. Fig. 6 shows a schematic of the arrangement. The cylinders can be packed tightly in the racks because only the sides need to be treated. The cylinder pairs are separated horizontally by 0.75-cm gaps, and vertically by ~1.1 cm of support structure and copper cooling lines. The total exposed area is over 16 m<sup>2</sup>. The racks are spaced 25 cm apart and centered in a cylindrical vacuum chamber that is 1.5 m in diameter and 4.6 m long. The racks are supported by ceramic insulators and are connected to the high-voltage feedthrough by a manifold constructed from stainless steel tubing. A cooling fluid runs through the target assembly to remove energy deposited by the implantation process and limit the target's temperature excursion.

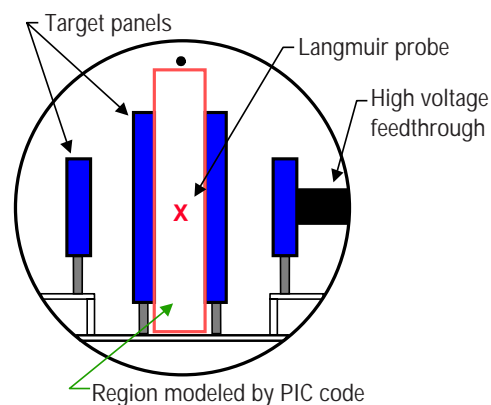


*Fig. 6 Schematic of the piston surrogate assembly, vacuum chamber, and Langmuir probe insertion position (shown by an "X" in the figure).*

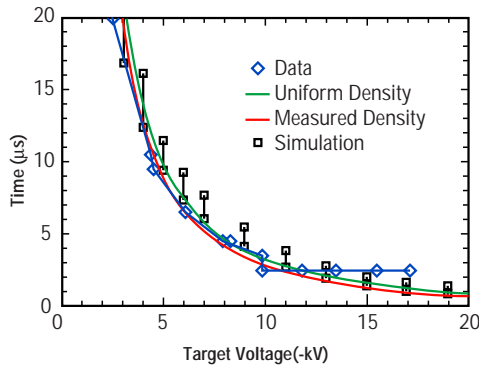


*Fig. 7 Sheath overlap times between the racks of pistons as a function of target voltage. The blue data points were measured with the center probe tip. The green line is from the Lieberman theory for uniform density plasma, and the red line is for a parabolic density profile. The black squares are from the simulation, showing the finite time for the electron density to drop to zero.*

To produce the background plasma, two  $3 \times 350$ -cm stainless steel radio frequency (RF) antennas are situated  $\sim 20$  cm from the top of the vacuum chamber. One is centered and the other is displaced approximately  $30^\circ$  from vertical. A separate 1000-W, 13.56-MHz RF generator and matching network drives each antenna. The two RF generators are phase-locked, and are operated at the same power output setting. Driving the antennas creates a capacitive RF discharge of density  $n \sim 10^8$  to  $10^9$   $\text{cm}^{-3}$ , with an estimated electron temperature,  $T_e$ , of  $\sim 3$  eV.<sup>13</sup> The electron distribution is not expected to be entirely Maxwellian, and probably contains a high energy tail.<sup>21</sup> In conventional systems, methane ( $\text{CH}_4$ ) is typically used as a working gas during the ion implantation step of making a diamond-like-carbon coating.<sup>10</sup> However, we used argon as the working gas to reduce complications from multiple ionic species and time-dependent surface conditions of Langmuir probe tips. Argon fill pressures used in these experiments ranged from 20 to 65 mPa.

A Langmuir probe assembly was inserted axially into the vacuum chamber and positioned between the two center racks (Fig. 6). The probe assembly was used to monitor basic plasma parameters, primarily plasma density, floating potential, and indications of plasma fluctuations. The probe was also used to determine the spatial characteristics of the plasma sheath expansion within the target assembly. To clarify the experimental results, the central portion of the target assembly was modeled using a two dimensional particle-in-cell (PIC) computer code (XPDP2, obtained from the Plasma Theory and Simulation Group at the University of California in Berkeley). The experimental configuration and modeling efforts are described in detail in two recent publications<sup>22,23</sup> and are summarized below.

In the interior portion of the assembly, the target racks appear essentially as quasi-planar structures and generate roughly planar plasma sheaths. If plasma density, applied target voltage, and voltage pulse duration are in the appropriate range (moderate plasma density, applied target voltages above a few kV, and pulse durations in excess of a few microseconds), these sheaths expand outward from the target racks and collide with each other on the planes dividing the racks. Measurements obtained from the Langmuir probe assembly allow a direct determination of the sheath overlap time (referenced to the start of the voltage pulse) for various experimental conditions. These measurements have been compared with sheath overlap times calculated from simple analytic theory, from a modification of the standard analytic theory to account for the measured variation of the plasma density in the sheath expansion region, and from results of the numerical PIC code. The comparison of these results is shown in Fig. 7. In general, the agreement is fairly good for the set of conditions of this measurement set. These conditions, however, minimize the impact of the secondary electrons on the background plasma and sheath propagation characteristics.

The strong interaction of the secondary electrons, target assembly, and background plasma appears in the form of two



different instabilities. The first, the “hollow cathode” instability, operates in much the same way as a hollow cathode discharge. Secondary electrons are temporarily trapped in the potential well between the racks of pistons, and directly ionize the background gas. The cross-section for ionization is enhanced by a reduction in the kinetic energy of the secondaries due to the overlap of the sheaths from adjacent racks of pistons so that this instability has significant impact only at low plasma densities and relatively high gas pressures. Furthermore, it occurs only if the secondary electron flux is sufficiently high. In experiments where a layer of graphite on the racks of pistons reduced the secondary electron emission coefficient, the instability was not observed until the graphite was sputtered off of the pistons. The hollow cathode instability effects are shown in Fig. 8.

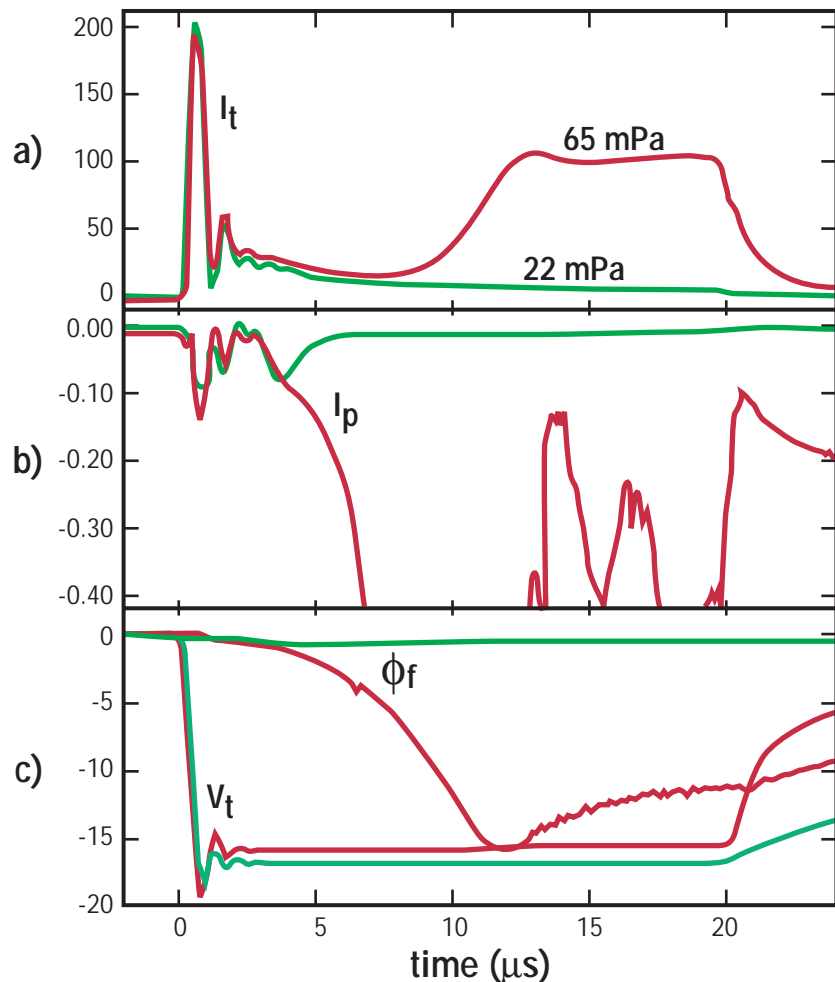
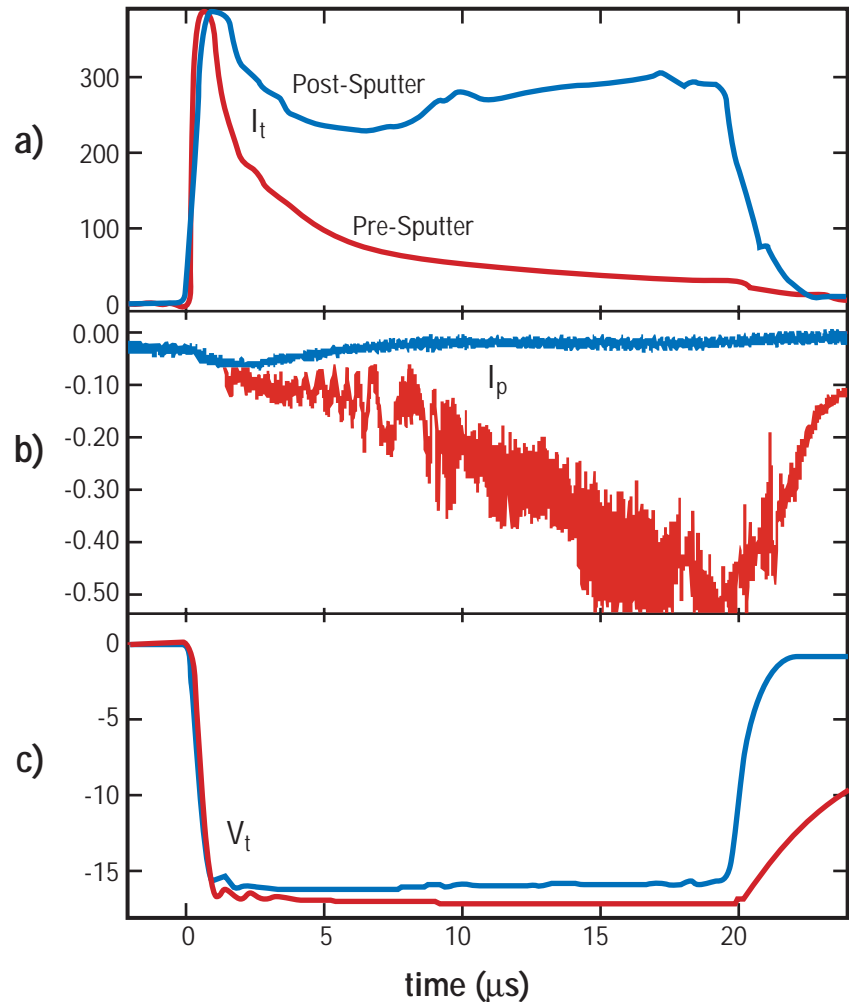


Fig. 8 Measurements of the (a) target current,  $I_t$ ; (b) probe current,  $I_p$ ; and (c) probe floating potential,  $\Phi_f$ , and target voltage,  $V_t$ , during the hollow cathode instability for 100 W of radio-frequency power. Negative currents signify the collection of electrons. The instability appears at 65 mPa fill pressure (red lines) but not at 22 mPa (green lines).

The second interaction mechanism is a beam-plasma instability, where the secondary electrons resonantly excite plasma waves. The energy in the plasma waves is transferred to the bulk plasma through Landau damping, causing an increase in the electron temperature and thereby an increase in the ionization rate. (A similar concept has been patented, but no experimental results have been published.) Unlike the hollow cathode instability, the beam-plasma instability requires a relatively large initial density. If the initial density is sufficiently large, the energy of the secondary electrons can be transferred to the bulk electrons before sheath overlap. The subsequent ionization of the background gas is then so rapid that the sheath motion is halted, preventing the sheaths from overlapping. A relatively high neutral gas pressure and a large flux of secondary electrons are also requirements for this instability to take hold. Impact of beam instability is illustrated in Fig. 9.

*Fig. 9 Measurements of the (a) target current,  $I_t$ ; (b) probe current,  $I_p$ ; and (c) target voltage,  $V_t$ , during the beam-plasma instability for 1,800 W of radio-frequency power and a gas pressure of 65 mPa. Negative currents signify the collection of electrons. The instability appears after sputter cleaning has increased the secondary electron flux (blue lines) but not before (red lines).*



## Conclusions

Successful commercial application of PSII depends on the ability to appropriately implant target components in a wide range of geometric configurations, particularly those in which the components have been relatively densely packed into a processing chamber. In our experiment, we explored the plasma sheath and plasma-target interaction characteristics within such a complex target assembly. This study yielded the first experimental demonstration of several important interaction mechanisms which are driven in the geometrically complex PSII system by the presence of energetic secondary electrons generated at the target surface by the implanted ions. Understanding these interactions will significantly increase our ability to predict the behavior of complex targets, and optimize target configurations for commercial application of PSII technology.

## References

- <sup>1</sup> R. J. Adler and S. T. Picraux, "Repetitively Pulsed Metal-Ion Beams for Ion Implantation," *Nuclear Instruments and Methods in Physics Research B* 6, 123 (1985).
- <sup>2</sup> J. R. Conrad and K. Sridharan (Eds.), "Papers from the First International Workshop on Plasma-Based Ion Implantation: August 4–6, 1993, University of Wisconsin," *Journal of Vacuum Science and Technology B* 12, 813 (1994).
- <sup>3</sup> G. A. Collins (Ed.), "Proceedings of the Second International Workshop on Plasma-Based Ion Implantation, Sydney, Australia, February 12–15, 1995," *Surface Coatings and Technology* 85, 28 (1996).
- <sup>4</sup> J. R. Conrad, "Sheath Thickness and Potential Profiles of Ion-Matrix Sheaths for Cylindrical and Spherical Electrodes," *Journal of Applied Physics* 62, 777 (1987).
- <sup>5</sup> J. R. Conrad, J. L. Radtke, R. A. Dodd, F. J. Worzla, and N. C. Tran, "Plasma Source Ion Implantation Technique for Surface Modification of Materials," *Journal of Applied Physics* 62, 4591 (1987).
- <sup>6</sup> J. R. Conrad, "Method and Apparatus for Plasma Source Ion Implantation," U.S. Patent No. 4,764,394 (August 16, 1988).
- <sup>7</sup> J. R. Conrad, "Plasma Source Ion Implantation: A New Approach to Ion-Beam Modification of Materials," *Materials Science and Engineering A* 116, 197 (1989).



- <sup>8</sup> D. J. Rej and R. B. Alexander, "Cost Estimates for Commercial Plasma Source Ion Implantation," *Journal of Vacuum Science and Technology B* 12, 2380 (1994).
- <sup>9</sup> D. J. Rej, "Plasma Source Ion Implantation," in M. Nastasi and J. W. Mayer (eds.), *Ion-Solid Interactions: Fundamentals and Applications*, Vol. I (Cambridge University Press, New York, 1996), p. 467.
- <sup>10</sup> C. P. Munson, R. J. Faehl, F. Henins, M. Nastasi, W. A. Reass, D. J. Rej, J. T. Scheuer, K. C. Walter, and B. P. Wood, "Recent Advances in Plasma Source Ion Implantation at Los Alamos National Laboratory," *Surface and Coatings Technology* 84, 528 (1996).
- <sup>11</sup> R. B. Alexander, "Using Ion Implantation to Improve Forming-Tool Life," *The Fabricator* 11, 1 (1992).
- <sup>12</sup> A. Chen, J. T. Scheuer, C. Ritter, R. B. Alexander, and J. R. Conrad, "Comparison between Conventional and Plasma Source Ion-Implanted Femoral Knee Components," *Journal of Applied Physics* 70, 6757 (1991).
- <sup>13</sup> M. A. Lieberman and A. J. Lichtenberg, *Principles of Plasma Discharges and Materials Processing* (Wiley-Interscience, New York, 1994).
- <sup>14</sup> S. B. J. Charter, L. R. Thompson, and G. Dearnaley, "The Commercial Development of Ion Implantation for Steel and Carbide Tools," *Thin Solid Films* 84, 355 (1981).
- <sup>15</sup> F. A. Smidt and D. B. Sartwell, "Manufacturing Technology Program to Develop a Production Ion Implantation Facility for Processing Bearings and Tools," *Nuclear Instruments and Methods in Physics Research B* 6, 70 (1985).
- <sup>16</sup> J. R. Treglio, A. J. Perry, and R. J. Stinner, "Economics of Metal Ion Implantation," in *Proceedings of the Eighth International Conference on Surface Modification of Metals by Ion Beams* (September 1993, Kanazawa, Japan) *Surface and Coatings Technology* 65, 184 (1994).
- <sup>17</sup> J. T. Scheuer, M. Shamim, and J. R. Conrad, "Model of Plasma Source Ion Implantation in Planar, Cylindrical, and Spherical Geometries," *Journal of Applied Physics* 67, 1241 (1990).

- <sup>18</sup> J. G. Andrews and R. H. Varley, "Sheath Growth in a Low-Pressure Plasma," *Physics of Fluids* 14, 339 (1971).
- <sup>19</sup> B. P. Wood, "Displacement Current and Multiple-Pulse Effects in Plasma Source Ion Implantation," *Journal of Applied Physics* 73, 4770 (1993).
- <sup>20</sup> M. Shamim, J. T. Scheuer, R. P. Fetherston, and J. R. Conrad, "Measurement of Electron Emission due to Energetic Ion Bombardment in Plasma Source Ion Implantation," *Journal of Applied Physics* 70, 4756 (1991).
- <sup>21</sup> V. A. Godyak, R. B. Piejak, and B. M. Alexandrovich, "Probe Diagnostics of Non-Maxwellian Plasmas," *Journal of Applied Physics* 73, 3657 (1993).
- <sup>22</sup> B. P. Cluggish and C. P. Munson, "Sheath Overlap During Very Large-Scale Plasma Source Ion Implantation," *Journal of Applied Physics* 84, 5937 (1998).
- <sup>23</sup> B. P. Cluggish and C. P. Munson, "Secondary-Electron Enhanced Discharges in Plasma Source Ion Implantation," *Journal of Applied Physics* 84, 5945 (1998).